JETP Letters, Vol. 80, No. 11, 2004, pp. 692–696. From Pis'ma v Zhurnal Éksperimental'noĭ i Teoreticheskoĭ Fiziki, Vol. 80, No. 11, 2004, pp. 819–823.

Strong Spin Triplet Contribution of the First Removal State in the Insulating Regime of $Bi_2Sr_2Ca_{1-x}Y_xCu_2O_{8+\delta}$¶

C. Janowitz[1], U. Seidel[1], R.-S. T. Unger[1], A. Krapf[1], R. Manzke[1], V. Gavrichkov[2], and S. Ovchinnikov[2]

[1] *Institute of Physics, Humboldt University of Berlin, 12489 Berlin, Germany*
[2] *Kirensky Institute of Physics, Russian Academy of Sciences, Krasnoyarsk, 660036 Russia*
e-mail: gav@iph.krasn.ru
Received October 6, 2004

The experimental dispersion of the first removal state in the insulating $Bi_2Sr_2Ca_{1-x}Y_xCu_2O_{8+\delta}$ regime is found to differ significantly from that of other parent materials: oxyclorides and La_2CuO_4. For Y contents of $0.92 \geq x \geq 0.55$ due to nonstoichiometric effects in the Bi–O layers, the hole concentration in the CuO_2 layers is almost constant and, on the contrary, the crystal lattice parameters *a*, *b*, *c* change very strongly. This (*a*, *b*) parameter increase and *c* parameter decrease results in an unconventional three peak structure at (0, 0), (π/2, π/2), (π, π) for $x = 0.92$. We can describe the experimental data only beyond the framework of the three-band *p–d*-model involving the representations of a new triplet counterpart for the Zhang–Rice singlet state. © *2004 MAIK "Nauka/Interperiodica".*

PACS numbers: 73.20.At; 74.25.Jb; 74.62.Dh; 79.60.Bm

Until now in high-T_c cuprates, there has not been any clear evidence that there is a contribution to the first removal state from states distinct from the Zhang–Rice singlet (ZRS) A_{1g} state. Early theoretical works [1–4] indicating the possible approach of the ZRS and the $^3B_{1g}$ two-hole states remained without any experimental support. Interestingly, the simple inversion of the triplet and singlet states should be accompanied by a change in the type of magnetic ordering already in undoped parent structures. The question on the type of magnetic ordering or magnetic and quasiparticle excitations spectra in the case of their approach has never been investigated since this problem cannot be studied within the framework of the three-band *p–d*- and *t–J*-models.

Accordingly, theoretical descriptions have been developed for antiferromagnetic (AF) insulators La_2CuO_4 and $Sr_2CuO_2Cl_2$ leading to states with the periodicity of the AF Brillouin zone [5, 6], i.e., maxima at $\mathbf{k} = (\pi/2, \pi/2)$. Our systematic high resolution ARPES (angle resolved photoemission) study of $Bi_2Sr_2Ca_{1-x}Y_xCu_2O_{8+\delta}$ ($x > 0.55$) shows additional new states at $\mathbf{k} = (0, 0)$ and $\mathbf{k} = (\pi, \pi)$. In contrast to La_2CuO_4, in $Bi_2Sr_2Ca_{1-x}Y_xCu_2O_{8+\delta}$, the hole concentration per Cu x_h is smaller than a substitution concentration *x* because some holes induced by $Ca^{+2} \longrightarrow Y^{+3}$ substitution go to the Bi–O layers. For example, in the insulator region $1 \geq x \geq 0.5$, the value n_h changes very weakly by $0.02 \leq n_h \leq 0.05$ [7]. Nevertheless, changes in the crystal lattice parameters are induced by the composition variable *x*, leading to an (*a*, *b*)-parameter increase and *c*-parameter decrease with increasing Y concentration *x* [8]. As a consequence, the hopping parameters t_{pp} (in-plane O–O hopping) and t'_{pp} (in-plane O–out-of-plane O hopping) also vary with the lattice parameters. Thus, in $Bi_2Sr_2Ca_{1-x}Y_xCu_2O_{8+\delta}$, at almost constant hole concentration, the reduction of the relation d_{pl}/d_{ap} (Cu–in-plane O and Cu–out-of-plane O distances) or so-called "chemical" pressure effect takes place. It is, according to [1–4], one of the main reasons for the approach of the singlet and triplet states. $Bi_2Sr_2Ca_{1-x}Y_xCu_2O_{8+\delta}$ single crystals were grown from the melt (for details see [9]). By replacement of the bivalent calcium with trivalent yttrium, the hole concentration of the CuO_2 planes has been controlled in the samples. The superconducting properties respectively the disappearance of superconductivity with doping were proven by susceptibility measurements. The stoichiometry and, in particular, the Y content were determined by energy dispersive X-ray analysis (EDX). For an Y content of $0.92 \geq x \geq 0.55$, the crystals showed no superconducting transition in susceptibility. The samples were rectangularly shaped with the long side along the crystallographic *a* axis, confirmed by diffraction experiments, and had a typical size of 5×2. Crystals were cleaved in UVH ($p = 1 \times 10^{-10}$ mbar) and were measured at a temperature of 90 K. No effects due to charging of the samples have been observed. LEED and Laue patterns revealed sharp spots for all doping concentrations. An example is given in Figs. 1d and 1e. Since all samples showed about a 1×5 reconstruction,

¶ This article was submitted by the authors in English.

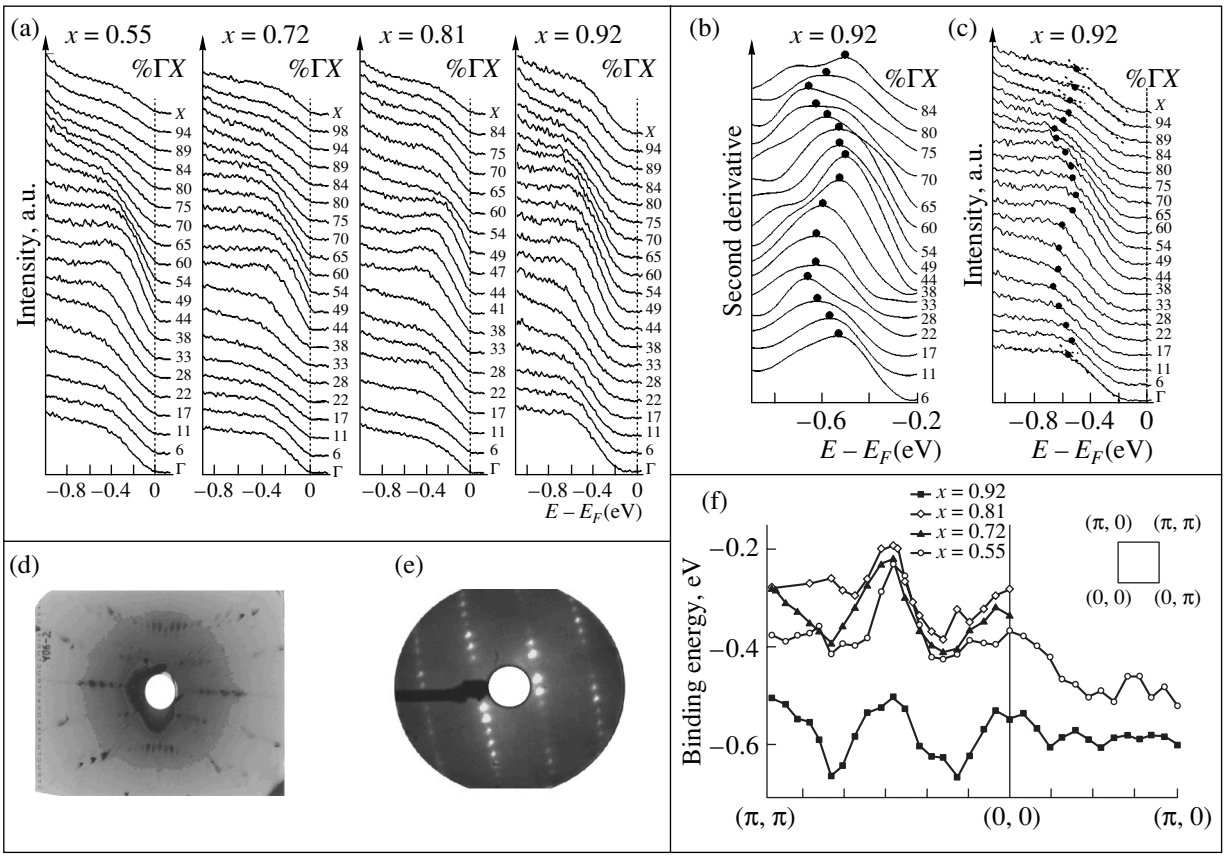

Fig. 1. (a) EDCs of $Bi_2Sr_2Ca_{1-x}Y_xCu_2O_{8+\delta}$ single crystals in the insulating phase taken along the Γ*X* (0, 0) ⟶ (π, π) direction of the Brillouin zone for different Y content at $T = 90$ K. With increasing Y concentration, the number of holes in the CuO_2 plane decreases. The polarization plane of the synchrotron radiation was in the Γ*M* (0, 0) ⟶ (π, 0) direction. (b) Second derivative of a selection of spectra from (c) multiplied by a factor of minus one. The maxima are marked by a dot. (c) Spectra along the Γ*X* direction of the sample with the highest Y concentration ($x = 0.92$). The positions of the centroids have been obtained either from the maxima of (b) (derivative method) or as the intersection of the tangents (tangent method). In the latter case, this has been indicated by two straight lines in (c). (d) Example of a typical LEED picture for a single crystal with Y concentration $x = 0.72$ at an electron energy of 70 eV. (e) Example of a typical Laue pattern for a single crystal with Y concentration $x = 0.72$. (f) Dispersion of the uppermost CuO derived states as obtained from the spectra of (a) along the major symmetry lines. The Γ*M* dispersions are from spectra not shown.

the spectra were recorded along the Γ*X* and not along the Γ*Y* direction to avoid contributions of superstructure bands. The ARPES experiments have been performed at the 3*m* normal-incidence monochromator HONORMI at beamline *W3.2* of HASYLAB. For the measurements discussed here, a photon energy of 18 eV was used. The energy distribution curves (EDC) were recorded with a hemispherical deflection analyzer with a total acceptance angle of 1° and an energy resolution of 10 meV [10]. Due to the broader emission maxima of insulating HTSCs, an overall resolution (analyzer plus monochromator plus temperature) of 80 meV was sufficient in order to improve statistics. An *AU* Fermi edge served as the Fermi energy reference.

Because the photoemission line shape of high temperature superconductors at arbitrary doping levels is not well understood, there is a strong need for a reliable data analysis procedure that gives a reasonable approximation of the real physics but does not lead to wrong conclusions. It is at present not known whether a spectrum for a given doping level can be interpreted in terms of single-particle excitations. The objective is, therefore, simply to define approximate quantities that reflect the energy scale of the data. The centroid (the center of gravity) of spectral features and positions of leading edges are the obvious possibilities. In the recent literature, a rather simple model consisting of a Lorentzian sitting on a step-edge background has been adopted to model the broad dispersing structures observed for insulating and underdoped cuprates [11]. It has been found [12] that, even in highly under-doped samples, the change in the slope of the spectra is a characteristic that easily identifies the broad high-energy feature. This procedure is illustrated in Fig. 1c by the dashed intersecting tangents, which approximate the up and down slope of the spectra (tangent method). It is thereby assumed that the steeper the slope, the closer the ZRS band to the Fermi energy. An alternative

method is to take the minima of the second derivative of the smoothed spectra (derivative method). This method to determine dispersion was, for instance, recently applied by Ronning *et al.* [5]. An example of this method is given in Fig. 1b, which shows a selection of second derivatives from the spectra of Fig. 1c (the derivatives were multiplied by minus one to obtain peaks). We used this method preferentially. Only in cases where the second derivatives came out too broad or as double structures, as was the case for the Γ spectrum and the three spectra at the highest angles from Fig. 1c, was the tangent method used. A comparison of both methods on the same spectra yielded approximately the same results. The intersection of the two slopes (tangent method) showed a systematic 30–60 meV shift to higher binding energies when compared to the derivative method. The typical error from the tangent method was 100 meV and from the derivative method between 60 meV and 100 meV. A detailed report will be given in a forthcoming publication.

In Fig. 1, series of spectra of the insulating state of the $Bi_2Sr_2Ca_{1-x}Y_xCu_2O_{8+\delta}$ single crystals are shown for the Γ*X* direction ((0, 0) ⟶ (π, π)) of the Brillouin zone (panel (a)). The origin of the dispersing spectral weight near the Fermi level is due to strongly correlated CuO states located in the CuO_2 planes. While for low Y content and optimum doped crystals with the highest T_c ($x \le 0.2$) the well-established Fermi level crossing is observed at about 0.4 Γ*X* (not shown), the insulators with $x \ge 0.55$ investigated here reveal no spectral weight at the Fermi energy. But the dispersing ZRS band is still present. The centroid of the ZRS bands of all insulators with Y content of $0.92 \ge x \ge 0.55$ is shifted to about the same binding energy of 300 meV. At a point halfway between Γ and (π, π), these insulators exhibit a distinct maximum in their dispersions, which is most pronounced for $x = 0.55$. With increasing *c* (decreasing hole concentration), the dispersion curves begin to rise around the (0, 0) and (π, π) points of the Brillouin zone.

A dramatic change is observed for the $x = 0.92$ insulator. The centroid of the band has now been shifted to about 600 meV, and instead of one dominating maximum in the dispersion curve, three equally strong maxima are observable at positions (0, 0), (π/2, π/2), and (π, π) of the Brillouin zone. While the 600 meV shift is hard to ascribe to a definite reason and is possibly due to pinning by defects [5], the appearance of this new state is exciting and new. Around $x = 0.92$, the insulator is supposed to cross the boundary from the non-AF insulating to the AF insulating phase. In the AF state, the next-nearest-neighbor copper atoms have antiparallel spin orientation coupled by a superexchange interaction via oxygen. The Wigner–Seitz cell then becomes twice as large and, as a consequence, the first Brillouin zone (BZ) is reduced by a factor of two and rotated by 45° [13]. If the underlying AF Brillouin zone were the only reason for the change in dispersion, the maximum at (π/2, π/2) as in the oxychlorides could be explained, but not the developing maxima at (0, 0) and (π, π). The above findings are therefore not similar to the observations in the oxychloride $Sr_2CuO_2Cl_2$ [5, 6, 14], which has been thought to behave like the parent compound of high-T_c cuprates. Despite the fact that the absolute maximum of the dispersion curve is also in $Sr_2CuO_2Cl_2$ at 0.5 Γ*X*, the band energy as well as the bandwidth are at variance with the insulating $Bi_2Sr_2Ca_{1-x}Y_xCu_2O_{8+\delta}$ samples.

All our attempts to obtain the three peaks in the dispersion at (0, 0), (π/2, π/2), and (π, π) in the framework of the *t*–*t*′–*t*″–*J* model failed. That is why we started with a more general model, the five-band *p*–*d*-model that takes into account Cu $d_{x^2-y^2}$, d_{z^2}, in-plane O p_x, p_y, and apical O p_z single-hole atomic states. The effect of strong electron correlations is certainly very important in the insulating phase, and in the framework of the multiband *p*–*d*-model, the generalized tight binding (GTB) method takes into account different intra-atomic Coulomb and Hund exchange interactions at Cu and O sites as well as Cu–O nearest neighbor repulsion. While in the three-band *p*–*d*-model the top of the valence band is formed by a dispersion of holes excited into the ZRS state, the new physics in the multiband *p*–*d*-model results from the $^3B_{1g}$ triplet contribution. The triplet counterpart for the ZRS is also known in the three-band *p*–*d*-model with energy much higher than the ZRS, $\Delta E = E_T - E_S \approx 2$ eV, so the triplet is not relevant in the low-energy region. This irrelevance appears to be a model-dependent result. In the multiband model presented here, Δ*E* sharply decreases due to Hund exchange contributions from the $d^{\uparrow}_{x^2-y^2}d^{\uparrow}_{z^2}$ configuration and additional bonding with apical oxygen-induced t'_{pd} and t'_{pp} hopping (here prime refers to the p_z apical orbital). For realistic parameters fitted well to the ARPES results for $Sr_2CuO_2Cl_2$ [15], the value $\Delta E \approx 0.7$ eV, and excitation of the extra hole added to b_{1g}, the initial state to the $^3B_{1g}$ triplet state gives a strong admixture near the (0, 0) and (π, π) points to the ZR singlet. To describe the ARPES in the insulating phase of $Bi_2Sr_2Ca_{1-x}Y_xCu_2O_{8+\delta}$, we take into account the strong lattice parameter dependence on the Y content (parameter *c* decreases and in-plane parameters *a*, *b* increase with the Y concentration *x* [8]) and neglect the small changes in the hole concentration. The corresponding changes of the in-plane oxygen t_{pp} hopping and the in-plane apical oxygen hopping t'_{pp} are given in the table.

Table

Y content	0	0.55	0.72	0.81	0.92
t_{pp}	0.45	0.35	0.34	0.33	0.32
t'_{pp}	0.42	0.44	0.45	0.47	0.48

For simplicity, the other model parameters are the same as in the undoped CuO_2 layer [15]. The dispersion of the top of the valence band for different Y concentration is then calculated by the *GTB* method and is shown in Fig. 2. With increasing Y content, the three-peak structure along the direction (0, 0) ⟶ (π, π) is clearly observed with the (π/2, π/2) peak slightly decreasing its energy. Along the (π, π) ⟶ (π, 0) line, there is no significant effect of the Y substitution. These results are in a good agreement with the ARPES data. Both states mix well to the one band of first removal states, in spite of the fact that there is a significant difference between them.

To clarify the triplet vs. singlet contribution, we have calculated the partial spectral weight contributions to the ARPES peaks (Fig. 3). The spectral function for the (π/2, π/2) peak is determined mostly by the singlet, as in the *t–J* model. The main contribution to the (0, 0) and (π, π) peaks is given by the triplet $^3B_{1g}$ and this contribution grows with increasing *x*. Figure 4 gives a comparison between experiment and theory for the dispersion of the crystals with the highest ($x = 0.92$) and lowest ($x = 0.55$) Y concentration along (0, 0) ⟶ (π, π). The spectrum for the $x = 0.92$ sample has been shifted to equal minimum binding energy with the $x = 0.55$ spectrum in the manner also applied by Ronning *et al.* [5]. It can be seen very clearly from Figs. 3 and 4 that the dispersion at (0, 0) and (π, π) changes considerably, because the new contribution of triplet states becomes detectable due to its increased spectral weight. To conclude, we have measured that, due to the "chemical" pressure effect induced by Y substitution in $Bi_2Sr_2Ca_{1-x}Y_xCu_2O_{8+\delta}$, the dispersion of the first removal state shows, at least near the AF phase at $x = 0.92$, a pronounced three-peak structure at the (0, 0), (π/2, π/2), (π, π) symmetric points of the BZ. Modeling the changes of the *a*, *b*, *c* lattice parameters in the GTB method with an essentially three-dimensional five-band *p–d* model, we reproduced the experimental three-peak structure and its concentration dependence. One may say our results indicate that the (0, 0) and (π, π) peaks result from the two-hole $^3B_{1g}$ counterpart for the Zhang–Rice state near E_F, which appears at far higher binding energies in two-dimensional three-band *p–d* models or *t–J* models.

Our data also support the earlier scenario [16, 17] that the dispersion along the (π/2, π/2) ⟶ (π, 0) direction is strongly reduced by the inclusion of the apical oxygen orbital, and its inclusion is absolutely essential for obtaining the weak dispersion observed experimentally. Thus, we offer a new testing ground for the theory of band structure in high-T_c cuprates.

We are grateful to Dr. D. Manske and Dr. I. Eremin for their hospitality during our visit to Berlin; Dr. S. Rogaschewski and Dr. H. Dwelk for the characterization of the crystals; and the staff of HASYLAB, especially Dr. P. Gurtler and Prof. M. Skibowski's group from the University of Kiel, for assistance with the measure-

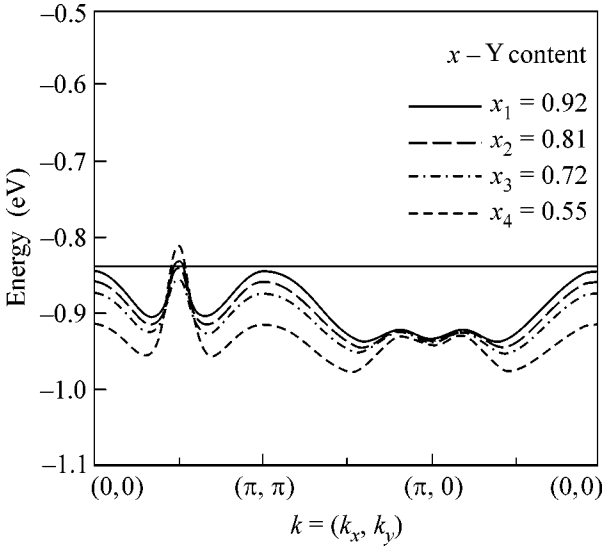

Fig. 2. The dispersion of the top of the valence band calculated by the GTB method for different Y contents *x*. *Y*(*x*) as indicated in the figure. The respective t_{pp} and t'_{pp} hopping parameters used for the calculations are given in table.

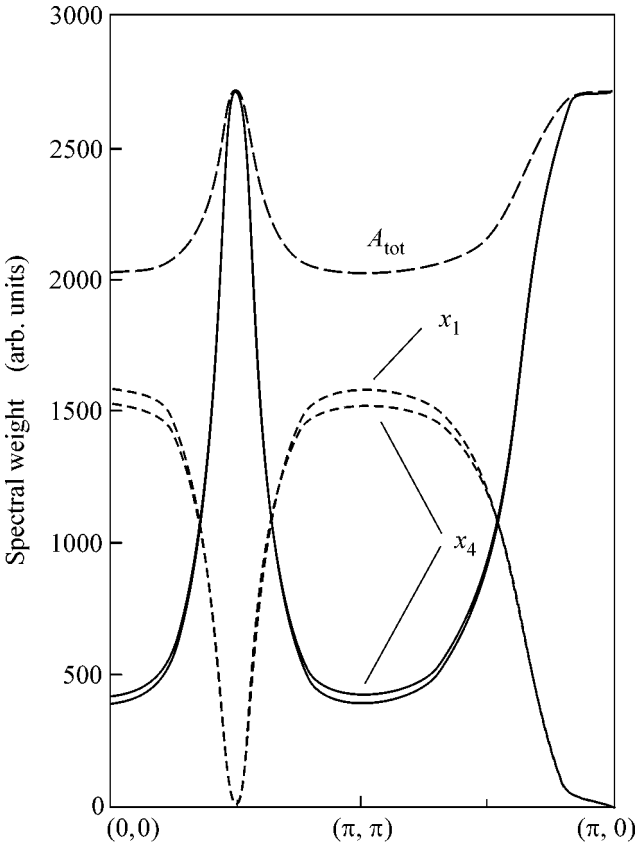

Fig. 3. Partial weights of the triplet states (dotted line) and singlet states (solid line) to A_{tot}—total spectral intensity at two different Y contents, $x_1 > x_4$. Here, the spectral function $A(\mathbf{k}, \omega)$ is taken along the peak positions in the $(\mathbf{k}, \omega)$ plane according to the dispersion shown in Fig. 1.

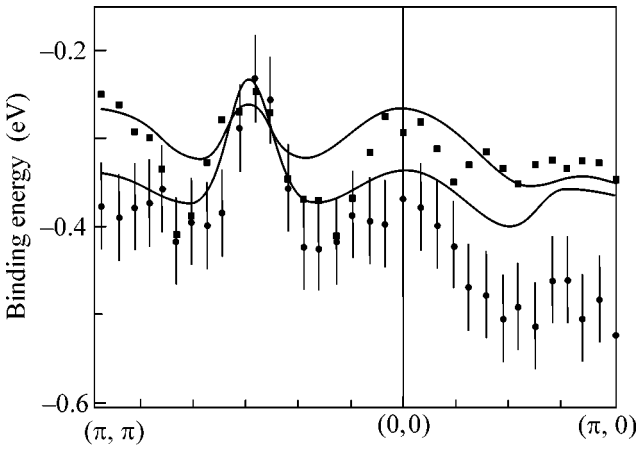

Fig. 4. Comparison of experimental (dots, $x = 0.55$; squares, $x = 0.92$) versus theoretical (dashed line, $x = x_4 = 0.55$; solid line, $x = x_1 = 0.92$ from Fig. 2) dispersions for the samples with the highest ($x = 0.92$) and lowest ($x = 0.55$) Y concentration along ΓX ((0, 0) $\longrightarrow$ (π, π)). The experimental $x = 0.92$ dispersion has been shifted to obtain a common valence band maximum with the $x = 0.55$ dispersion (see also the text).

ments. This work was supported by INTAS (grant no. 01-0654), the Russian Foundation for Basic Research (project no. 03-02-16124), the program of the Physics Branch of the Russian Academy of Sciences "Strongly Correlated Electron Systems," and the BMBF (project no. 05 KS1KH11).

REFERENCES

1. H. Kamimura and M. Eto, J. Phys. Soc. Jpn. **59**, 3053 (1990).
2. M. Eto and H. Kamimura, Physica C (Amsterdam) **185–189**, 1599 (1991).
3. H. Eskes *et al.*, Phys. Rev. B **41**, 288 (1990).
4. V. A. Gavrichkov and S. G. Ovchinnikov, Fiz. Tverd. Tela (St. Petersburg) **40**, 184 (1998) [Phys. Solid State **40**, 163 (1998)].
5. F. Ronning *et al.*, Phys. Rev. B **67**, 035113 (2003) and references therein.
6. C. Durr *et al.*, Phys. Rev. B **63**, 014505 (2001) and references therein.
7. M. Karpinnen *et al.*, Phys. Rev. B **67**, 134522 (2003).
8. C. Janowitz *et al.*, Czech. J. Phys. **47**, 403 (1997).
9. C. Janowitz *et al.*, Physica B (Amsterdam) **259**, 1134 (1999).
10. K. Rossnagel *et al.*, Nucl. Instrum. Methods Phys. Res. A **467**, 1485 (2001).
11. D. S. Marshall *et al.*, Phys. Rev. Lett. **76**, 4841 (1996).
12. J. C. Campuzano *et al.*, Phys. Rev. Lett. **83**, 3709 (1999).
13. P. Aebi *et al.*, Phys. Rev. Lett. **72**, 2757 (1994).
14. B. O. Wells *et al.*, Phys. Rev. Lett. **74**, 964 (1995).
15. V. A. Gavrichkov *et al.*, JETP **91**, 369 (2000); Phys. Rev. B **64**, 235124 (2001).
16. J. B. Grant and A. K. McMahan, Phys. Rev. B **46**, 8440 (1992).
17. R. Raimondi *et al.*, Phys. Rev. B **53**, 8774 (1996).